A Self-Building and Cluster-Based Cognitive Fault Diagnosis System for Sensor Networks

Cesare Alippi, *Fellow, IEEE*, Manuel Roveri, *Member, IEEE*, and Francesco Trovò, *Member, IEEE*

I. Introduction

FAULT diagnosis systems (FDSs) are tools designed to detect, isolate, identify, and, possibly, mitigate the occurrence of faults affecting complex systems. FDSs have been subject of extensive research for their relevance in real-world applications, see [1]–[4] for a comprehensive review. In their traditional framework, it is required the availability of the fault-free nominal state and a fault dictionary, containing the fault signatures. Both requests constitute a strong demand, hard to be met in most of real-world applications.

A novel and promising cognitive approach aims at designing FDSs able to automatically learn the nominal and the faulty states online, during the operational modality. Cognitive approaches generally rely on machine learning techniques to configure the nominal state and create the faulty ones without requiring any *a priori* information about the fault signature or on fault time profile [1], [5].

Most of existing cognitive FDSs apply the learning mechanism only during the configuration phase [6]–[9], thus requesting availability of the fault dictionary at training time. More in detail, [6] presents a learning methodology for incipient failure detection based on online approximators aiming at both inspecting variations in the system due to faults and providing information about the detected faults in an online manner. In [7], a learning procedure for fault accommodation is given, under the assumption that the process is linear. Reference [10] presents a scheme for online adaptive fault detection and accommodation. There, it is requested that the nominal fault-free state of the system is known. Differently from previous solutions, which confine the cognitive aspect solely to the training phase (hence not allowing the FDS to improve the fault dictionary during the operational life), [1] suggests the use of an unsupervised clustering-labeling method to automatically assign observations either to the nominal or the faulty class. Unfortunately, no technical details about the implementation of the solution are given.

There is a large literature addressing the design of cognitive FDSs for specific applications [8], [9], [11]–[20], with cognitive mechanisms mostly applied during the training phase of the FDS. For example, [9] presents a supervised method for fault classification, which exploits a recursive learning of a radial basis function network in chemical processes. Reference [8] suggests a cluster-labeling approach based on self-organizing maps for fault diagnosis applied to a quality inspection of tape deck chassis. Reference [11] describes an FDS specifically designed for fault isolation in power transformers based on evolving neural networks. Yang *et al.* [12] propose an intelligent FDS for electric motors based on ART-Kohonen neural networks: new faults can be included in the dictionary thanks to the design of a case-based reasoning learning system. Several FDSs based on fuzzy neural networks have been presented in [13]–[20], mainly addressing specific applications (e.g., bearing [14], induction motors [15], transformers [16], [17], marine propulsion engines [18], gearboxes [19], and circuit transmission [20]), while [13] suggests a fault identification technique based on the joint use of a fuzzy logic and feedforward neural networks. All presented methods are either application specific or request availability of the fault dictionary, strong assumptions that we relax in the sequel.

More in detail, this paper presents a cognitive FDS working in the parameter space of linear time-invariant (LTI) models approximating the investigated process dynamics over time. The proposed FDS, which extends the solution presented in [21], relies on a novel evolving-clustering algorithm (ECA) able to learn the nominal state of the process during an initial training phase and create, update, and maintain the fault

Manuscript received June 26, 2013; revised January 24, 2014; accepted January 27, 2014. Date of publication April 1, 2014; date of current version May 15, 2014. This work was supported by the European Commission's 7th Framework Program under Grant INSFO-ICT-270428.

The authors are with the Dipartimento di Elettronica, Informazione e Bioingegneria, Politecnico di Milano, Milan 20133, Italy (e-mail: alippi@elet.polimi.it; roveri@elet.polimi.it; trovo@elet.polimi.it).

dictionary automatically during the operational life. During the training phase, the cognitive FDS characterizes the nominal fault-free state and, in the following operational phase, assesses approximating models by labeling them as fault free, instances of a new faulty class or outliers. A sound theoretical framework justifies the use of approximating linear models to detect changes.

The main contributions of this paper can be summarized as proposing:

1) the design of an evolving FDS based on an adaptive clustering algorithm working in the space of approximating model parameters, able to characterize faults whose effect induces an abrupt change in the model parameters;
2) the theoretical justification for the use of a sequence of LTI models approximating the (possibly) nonlinear dynamic system within a fault diagnosis framework;
3) an ECA that takes advantage of temporal and spatial dependencies of the estimated parameters, whereas clustering solutions present in the literature usually consider only the spatial aspect, see [22]–[25].

The structure of this paper is as follows. Section II reviews the theoretical framework justifying the use of LTI models as building blocks to construct the cognitive FDS. Section III introduces the proposed cognitive FDS and Section IV details the aspects related to the online creation of the fault dictionary. Experimental results on both synthetic and real data sets are presented and discussed in Section V. Concluding remarks are finally given in Section VI.

II. Problem Formulation

In the following, we consider a time-invariant dynamic system whose model description is unavailable and a sensor network acquiring scalar measurements—or datastreams—from the system. Selection of the most appropriate placement for the sensors is outside the scope of this paper (the interested reader can refer to [26]–[29] for a comprehensive investigation of the displacement problem). We assume that changes in the system can be detected by inspecting changes in the functional relationships among sensor data. Each relationship between two generic sensors is described as presented in the sequel and the final decision about the change detection is taken at the network level, by relying on the framework proposed in [30].

In the following, each sensor-to-sensor relationship is modeled as a single time-invariant process $\mathcal{P}$ (extension to relationships described by a finite set of nonoverlapping processes $\{\mathcal{P}_1, \ldots, \mathcal{P}_\psi\}$ is immediate) and is approximated with an LTI predictive model belonging to a family $\mathcal{M}$ parametrised in $\theta \in \mathcal{D}_\mathcal{M}$, $\mathcal{D}_\mathcal{M} \subset \mathbb{R}^p$ being a compact C^1 manifold. MISO linear predictive models [31], extreme learning machines [32], and reservoir computing networks [33] are valuable instances for $\mathcal{M}$. In this paper, we opt for linear one-step-ahead predictive models in the form

$$\hat{y}(t|\theta) = f(t, \theta, u(t), \ldots, u(t-\tau_u), y(t-1), \ldots, y(t-\tau_y)) \quad \forall t \in \mathbb{N}$$

where $f(\cdot) \in \mathbb{R}$ is the approximating function in predictive form [34], e.g., ARX and ARMAX, $u(t) \in \mathbb{R}^m$ and $y(t) \in \mathbb{R}$ are the model input and output at time t, respectively, and τ_u and τ_y are the orders of the input and output, respectively. Given a training sequence composed of N couples $Z_N = \{(u(t), y(t))\}_{t=1}^N$ and a quadratic loss function, we define the structural risk [34] to be

$$W_N(\theta) = \frac{1}{N}\sum_{t=1}^{N} \mathbb{E}_{(u,y)}[\varepsilon^2(t,\theta)]$$

and the empirical risk as

$$V_N(\theta) = \frac{1}{N}\sum_{t=1}^{N} \varepsilon^2(t,\theta)$$

where $\varepsilon(t,\theta) = y(t) - \hat{y}(t|\theta)$ is the prediction error at time t. The optimal parameter $\theta^o \in \mathcal{D}_\mathcal{M}$ is defined as

$$\theta^o = \arg\min_{\theta\in\mathcal{D}_\mathcal{M}} \left[\lim_{N\to+\infty} W_N(\theta)\right].$$

An estimate $\hat{\theta} \in \mathcal{D}_\mathcal{M}$ of θ^o can be obtained by minimizing the empirical risk

$$\hat{\theta} = \arg\min_{\theta\in\mathcal{D}_\mathcal{M}} V_N(\theta). \tag{1}$$

By relying on the theoretical framework developed in [34] and [35], under the mild hypotheses that recent past data suffice to generate accurate approximations of $u(t)$ and $y(t)$, that $f(\cdot)$ is three time differentiable with respect to θ, and satisfies Lipschitz conditions, and that the structural risk is a convex function in $\mathcal{D}_\mathcal{M}$, minimization of $W_N(\theta)$ provides a unique point θ^o such that

$$\lim_{N\to\infty} \hat{\theta} = \theta^o \quad w.p.\ 1$$

and

$$\lim_{N\to\infty} \sqrt{N}\Sigma_N^{-\frac{1}{2}}(\hat{\theta} - \theta^o) \sim \mathcal{N}(0, I_p) \tag{2}$$

where

$$\begin{aligned}\Sigma_N &= \left[W_N''(\theta^o)\right]^{-1} U_N \left[W_N''(\theta^o)\right]^{-1} \\ U_N &= N\mathbb{E}\left[V_N'(\theta^o) V_N'(\theta^o)^T\right]\end{aligned}$$

and I_p is the identity matrix of order p.

The above result assures that, given a sufficiently large N, the estimated parameter vector $\hat{\theta}$ follows a multivariate Gaussian distribution with mean θ^o and covariance matrix Σ_N. Interestingly, the results presented in Section II contemplate the situation where $\mathcal{P} \notin \mathcal{M}$, i.e., a model bias $||\mathcal{M}(\theta^o) - \mathcal{P}|| \neq 0$ is present. This justifies the use of LTI models even when the dynamic system under investigation is nonlinear. According to (2), estimated parameters $\hat{\theta}$ follow a multivariate Gaussian distribution both approximating linear and nonlinear systems, provided that a sufficiently large data set is available. We emphasize that, in what follows, we are not interested in providing a high approximation accuracy, since LTI models are not used for prediction purposes (where nonlinearities in the system might induce a high prediction error) but for fault diagnosis ones. Parameter vectors are the features to be used for fault diagnosis and, since a change in the probability density function of the parameter features is associated with structural changes in the process generating the data (and nonlinearity does not introduce structural changes), we can design an FDS based on an ECA operating in the parameter space.

Although the nonlinearity aspect is contemplated by the theory, we might experience numerical problems in correspondence with an ill conditioned Hessian W_N'', e.g., following highly correlated inputs. However, we must comment that if W_N'' degenerates in rank then, given the linearity assumption for the considered approximation model, we should simply remove the linear dependent variables. In the case, we wish to keep them for the (small) innovation they provide, a Levenberg–Marquardt correction $W_N'' + \delta I_p$ (δ being a small positive scalar) should be introduced to grant a definite positive Hessian.

III. Cognitive FDS

The FDS relies on an initial training phase needed to characterize the nominal state Ψ by exploiting a fault-free training sequence $Z_M = \{(u(t), y(t))\}_{t=1}^{M}$. Z_M is then windowed into nonoverlapping batches of length N, each of which used to provide a parameter vector estimate $\hat{\theta}$. The outcome is the sequence $\Theta_L = (\hat{\theta}_1, \ldots, \hat{\theta}_i, \ldots, \hat{\theta}_L)$, $L = M/N$.

The proposed cognitive FDS is given in Algorithm 1. From the results delineated in Section II parameter vectors in Θ_L are distributed according to the Gaussian distribution, provided that N is large enough, even though the system is nonlinear. Thanks to (2), the nominal state Ψ can be described as a Gaussian cluster composed by equivalent models (each cluster point is a model), whose mean vector $\bar{\theta}_\Psi$ and covariance matrix S_Ψ can be estimated on Θ_L (Line 1). For cognitive diagnosis purposes, we assign to the nominal state also the number n_Ψ of parameter vectors used to estimate $\bar{\theta}_\Psi$ and S_Ψ and the last time instant t_Ψ for which a $\hat{\theta}_i$ was associated to the nominal state Ψ. At the end of the training phase, $n_\Psi = L$ and $t_\Psi = L$ (Line 2). The extension to multiclass nominal states, e.g., representing different regimes of $\mathcal{P}$, would require considering a set of Gaussian clusters for Ψ.

During the operational life, the proposed FDS estimates parameter vectors from incoming nonoverlapping N-sample data windows. The corresponding $\hat{\theta}_i s$ are then either associated to the nominal state Ψ or a generic jth faulty one Φ_j present in the fault dictionary $\Phi = \{\Phi_1, \ldots, \Phi_\phi\}$ (ϕ represents the number of current fault classes in the fault dictionary). If the assignment cannot be granted according to a given confidence level, the parameter vector is currently considered to be an outlier and moved to the outlier set O.

At the beginning, both the fault dictionary and the outlier set are empty [Fig. 1(a)] and are populated during the operational phase, as data come in. The outlier set is regularly inspected to determine whether a new state $\Phi_{\phi+1}$ has been there contained and needs to be generated [Fig. 1(b)]. If a parameter vector cannot be associated to either the nominal state or one of the faulty states according to the given confidence level, it is considered an outlier and moved to the outlier set O [see the asterisks near the ellipse in the upper right side of Fig. 1(d)]. Similarly, other housekeeping operations are executed on the

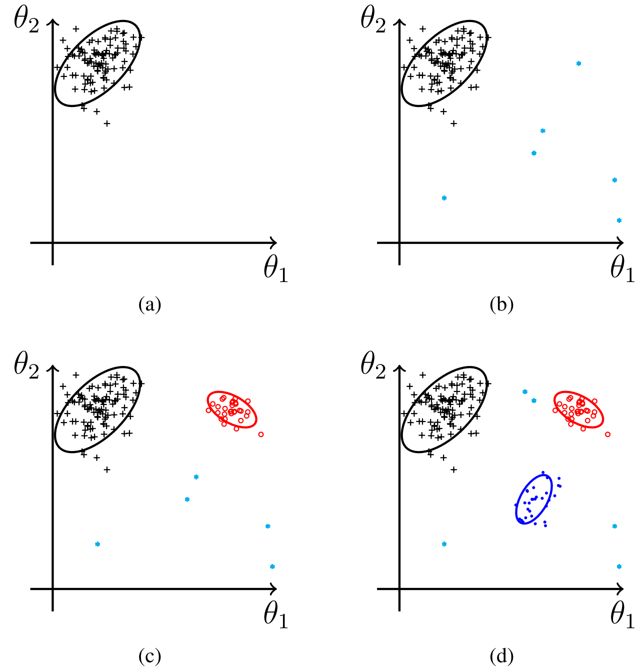

Fig. 1. Cognitive FDS: an example. (a) Nominal state (crosses) is characterized during the training phase. (b) Number of outliers (asterisks) is increasing but no faults are identified yet. (c) As soon as enough confidence is gathered for the presence of a new faulty state, a new cluster is created (circles) and instances added to it. (d) When a different fault is identified (dots), it is added to the fault dictionary.

existing structures (outlier and faulty sets), e.g., leading to the merge of two faulty states, whenever appropriate.

Details about the cognitive FDS algorithm are given in the sequel, while the creation of the fault set deserves a deeper discussion (Section IV).

Here, we assume that a fault affecting θ^o abruptly moves the process from a stationary state to a new stationary one (abrupt fault). A faulty state Φ_j is hence characterized by a mean vector $\bar{\theta}_{\Phi_j}$ and a covariance matrix S_{Φ_j}. The FDS stores the number n_{Φ_j} of vectors used to estimate $\bar{\theta}_{\Phi_j}$ and S_{Φ_j} and the latest time instant t_{Φ_j}, where $\hat{\theta}_i$ was associated to Φ_j.

The distance between a parameter vector $\hat{\theta}_i$ and the center of a cluster can be computed by means of the Mahalanobis distance

$$m(\hat{\theta}_i, \Upsilon) = (\bar{\theta}_\Upsilon - \hat{\theta}_i)^T S_\Upsilon^{-1} (\bar{\theta}_\Upsilon - \hat{\theta}_i)$$

where $\Upsilon \in \{\Psi, \Phi_1, \ldots, \Phi_\phi\}$. Since Ψ and $\Phi_j \in \Phi$ are Gaussian clusters, a neighborhood centered in $\bar{\theta}_\Upsilon$ can be induced by containing those $\hat{\theta}_i$s belonging to Υ with probability $1-\alpha_s$ [36], where α_s is a given confidence level. More specifically, the spatial neighborhood is composed by those θs for which

$$\frac{n_\Upsilon(n_\Upsilon - p)}{p(n_\Upsilon^2 - 1)} m(\theta, \Upsilon) \leq F_{p, n_\Upsilon - p, \alpha_s} \quad (3)$$

hold. $F_{p,n_\Upsilon-p,\alpha_s}$ is the Fisher's distribution quantile of order $1-\alpha_s$ of parameters p and $n_\Upsilon - p$. Similarly, a neighborhood is assigned to each cluster $\Upsilon \in \{\Psi, \Phi_1, \ldots, \Phi_\phi\}$ and constitutes the core of the fault identification phase of the FDS (Lines 6 and 14). The FDS algorithm also contemplates the case of $\hat{\theta}_i$ satisfying (3) for multiple clusters. In this case, $\hat{\theta}_i$ is associated

Algorithm 1 FDS ECA

1 Compute mean $\bar{\theta}_\Psi$ and covariance matrix S_Ψ for the nominal state cluster;
2 Set $n_\Psi = L$ and $t_\Psi = L$;
3 Set $\Phi = \emptyset$ ($\phi = 0$) and $O = \emptyset$;
4 Set α_s, η_t;
5 **while** *a new* $\hat{\theta}_i$ *is available* **do**
6   **if** *3 holds for at least one* $\Psi_j \in \Psi$ **then**
7   Select Ψ^* minimizing 4;
8   Associate $\hat{\theta}_i$ to Ψ^* ;
9   **if** $|t_\Psi - i| \leq \eta_t$ **then**
10   Update Ψ as in 6-8;
11   **end**
12     $t_{\Psi^*} \leftarrow i$;
13   **else**
14   **if** $\phi > 0$ *and 3 holds for at least one* $\Phi_j \in \Phi$ **then**
15   Select Φ^* minimizing 4;
16   Associate $\hat{\theta}_i$ to Φ^* ;
17   **if** $|t_{\Phi^*} - i| \leq \eta_t$ **then**
18   Update Φ^* as in 6-8;
19   **for** $\hat{\theta}_h \in O$ **do**
20   **if** *3 holds for* Φ^* **then**
21   Remove $\hat{\theta}_h$ from outlier set O ;
22   Associate $\hat{\theta}_h$ to Φ^* ;
23   **if** $|t^*_\Phi - h| \leq \eta_t$ **then**
24   Update Φ^* as in 6-8;
25   **end**
26   **end**
27   **end**
28   **for** $\Phi_j \in \Phi, \Phi \neq \Phi^*$ **do**
29   **if** *9 and 10 hold for* Φ^*, Φ_j **then**
30   Merge Φ^*, Φ_j as in 11-14;
31   **end**
32   **end**
33   **end**
34       $t_{\Phi^*} \leftarrow i$;
35   **else**
36   Insert $\hat{\theta}_i$ in O;
37   Create $\bar{O}$ according to Algorithm 2;
38   **if** $\bar{O} \neq \emptyset$ **then**
39         $\phi \leftarrow \phi + 1$;
40   Create Φ_ϕ using $\hat{\theta}_k \in \bar{O}$;
41   **end**
42   **end**
43   **end**
44 **end**

to the cluster Υ^* (either nominal of faulty, Lines 8 and 16) minimizing

$$\Upsilon^* = \min_{\Upsilon \in \{\Psi, \Phi_1, \ldots, \Phi_\phi\}} \frac{n_\Upsilon (n_\Upsilon - p)}{p(n_\Upsilon^2 - 1)} m(\hat{\theta}_i, \Upsilon). \tag{4}$$

In other words $\hat{\theta}_i$ is assigned to the nearest cluster, provided that confidence α_s is attained. Once Υ^* has been determined, we set $t_{\Upsilon^*} = i$ (Lines 12 and 34). If $\hat{\theta}_i$ cannot be associated either to Ψ, or to $\{\Phi_1, \ldots, \Phi_\phi\}$, it is considered to be an outlier and inserted in O (Line 36).

The algorithm, after taking into account the spatial locality between parameter vectors, analyzes the temporal one, by evaluating to which level recent $\hat{\theta}$s have been associated to Υ^* (Lines 9 and 17)

$$|n_{\Upsilon^*} - i| \leq \eta_t \tag{5}$$

where $\eta_t \in \mathbb{N}$ is a temporal threshold (when $\eta_t = 1$ the FDS verifies if two consecutive time vectors $\hat{\theta}_i$ and $\hat{\theta}_{i-1}$ have been assigned to the same cluster). This operation is important since we expect models built over time to be temporally dependent.

If $\hat{\theta}_i$ satisfies both the spatial (3) and the temporal (5) membership conditions, for cluster Υ^*, it is inserted in there and its statistics are updated, since a new instance has been received (Lines 10 and 18)

$$\bar{\theta}_{\Upsilon^*} \leftarrow \frac{n_{\Upsilon^*}}{n_{\Upsilon^*} + 1} \bar{\theta}_{\Upsilon^*} + \frac{1}{n_{\Upsilon^*} + 1} \hat{\theta}_i \tag{6}$$

$$S_{\Upsilon^*} \leftarrow \frac{n_{\Upsilon^*} - 1}{n_{\Upsilon^*}} S_{\Upsilon^*} + \frac{n_{\Upsilon^*} + 1}{n_{\Upsilon^*}^2} (\hat{\theta}_i - \bar{\theta}_{\Upsilon^*})(\hat{\theta}_i - \bar{\theta}_{\Upsilon^*})^T \tag{7}$$

$$n_{\Upsilon^*} \leftarrow n_{\Upsilon^*} + 1. \tag{8}$$

The aforementioned procedure might update cluster Υ_j so that it partly overlaps with another one Υ_k. The algorithm handles the situation with a cluster merging procedure (Lines 29–31). The union of clusters Υ_j and Υ_k is performed if the following two conditions are jointly satisfied

$$\frac{n_{\Upsilon_j}(n_{\Upsilon_k} n_{\Upsilon_j} - n_{\Upsilon_k} - p + 1)}{(n_{\Upsilon_k} + 1)(n_{\Upsilon_j} - 1) p} m(\bar{\theta}_{\Upsilon_j}, \Upsilon_k) \leq F_{p, n_{\Upsilon_k} n_{\Upsilon_j} - n_{\Upsilon_k} - p + 1, \frac{\alpha_m}{2}} \tag{9}$$

$$\frac{n_{\Upsilon_k}(n_{\Upsilon_j} n_{\Upsilon_k} - n_{\Upsilon_j} - p + 1)}{(n_{\Upsilon_j} + 1)(n_{\Upsilon_k} - 1) p} m(\bar{\theta}_{\Upsilon_k}, \Upsilon_j) \leq F_{p, n_{\Upsilon_j} n_{\Upsilon_k} - n_{\Upsilon_j} - p + 1, \frac{\alpha_m}{2}} \tag{10}$$

i.e., if the cluster means $\bar{\theta}_{\Upsilon_j}, \bar{\theta}_{\Upsilon_k}$ have probability greater than $1 - \alpha_m$ to belong (to be drawn from) each other clusters. In (9) and (10), $F_{p, n_{\Upsilon_k} n_{\Upsilon_j} - n_{\Upsilon_k} - p + 1, \alpha_m/2}$ is the Fisher's distribution quantile of order $1 - \alpha_m/2$, with parameters p and $n_{\Upsilon_k} n_{\Upsilon_j} - n_{\Upsilon_k} - p + 1$. Approximated results for the confidence α_m follow from the Bonferroni correction for multiple tests. If the above conditions are satisfied, the FDS merges the two clusters Υ_j and Υ_k to generate cluster Υ' defined as

$$\bar{\theta}_{\Upsilon'} \leftarrow \frac{n_{\Upsilon_j}}{n_{\Upsilon_j} + n_{\Upsilon_k}} \bar{\theta}_{\Upsilon_j} + \frac{n_{\Upsilon_k}}{n_{\Upsilon_j} + n_{\Upsilon_k}} \bar{\theta}_{\Upsilon_k} \tag{11}$$

$$S_{\Upsilon'} \leftarrow S_{\Upsilon_j} + S_{\Upsilon_k} + \frac{n_{\Upsilon_j} n_{\Upsilon_k}}{n_{\Upsilon_j} + n_{\Upsilon_k}} (\bar{\theta}_{\Upsilon_j} - \bar{\theta}_{\Upsilon_k})(\bar{\theta}_{\Upsilon_j} - \bar{\theta}_{\Upsilon_k})^T \tag{12}$$

$$n_{\Upsilon'} \leftarrow n_{\Upsilon_j} + n_{\Upsilon_k} \tag{13}$$

$$t_{\Upsilon'} \leftarrow \max\{t_{\Upsilon_j}, t_{\Upsilon_k}\}. \tag{14}$$

The exact computation of the update for the covariance matrix is performed as in [37].

After a cluster update or the merge of two clusters, the proposed FDS checks if parameter vectors in the outlier set O can now be associated either to the nominal state or one of the faulty ones (Lines 19–27).

IV. Online Characterization of the Fault Dictionary

We addressed so far the procedure allowing the insertion of the parameter vectors in the nominal and faulty clusters and the merging of two faulty clusters. The remaining $\hat{\theta}_i$ are collected in the outlier set O, where further inspection is performed during the operational phase, to verify whether a new faulty state must be created or not.

With reference to Algorithm 2, a new cluster needs to be created depending on the outcome of the Kolmogorov–Smirnov (KS) test (Line 4). The test compares the empirical cumulative distribution function (CDF) of all the $\hat{\theta}$s estimated by the FDS during both the training and the operational phases and the CDF induced by considering the estimated nominal state Ψ and faults $\{\Phi_1, \ldots, \Phi_\phi\}$. If the distribution of the $\hat{\theta}$s is no more coherent with the current set of clusters, a new cluster must be created and a new fault class inserted in Φ. More in detail, the test is designed as

$$H_0 : \hat{F} = F_\Gamma \text{ versus } H_1 : \hat{F} \neq F_\Gamma$$

where $\hat{F}$ is the empirical CDF of all the $\hat{\theta}$s and F_Γ is the distribution induced by Gaussian clusters $\Gamma = \{\Psi, \Phi_1, \ldots, \Phi_\phi\}$. The KS test statistics takes into account the maximum distance between the two CDFs

$$D^p = \max_{0 \leq \alpha \leq 1} |\hat{F}(B_\alpha) - F_\Gamma(B_\alpha)|$$

where B_α is the region in the parameter space such that $F_\Gamma(B_\alpha) = \alpha$ (see [38] for further details). As stated in [38], D^p has the same distribution of the monodimensional KS distribution, so, for the KS test, we can compare it with the asymptotic form of the KS distribution K [39], [40]. Given a confidence level α_c, the critical region of the KS test (i.e., for rejecting the null hypothesis H_0) is

$$D^p > K_{\alpha_c} \tag{15}$$

where K_{α_c} is the quantile of order $1 - \alpha_c$ of the monodimensional K distribution. The proposed statistical test suffers from the curse of dimensionality, i.e., it needs an exponentially increasing number of samples to be effective as the parameter vector dimension p increases. Therefore, if needed, we suggest to apply a dimensionality reduction method to the parameter vectors $\hat{\theta} \in O$, e.g., based on principal component analysis [36] or random projection method [41].

Once the KS test provides enough confidence to claim that a new cluster must be generated from the outlier set (i.e., hypothesis H_0 is rejected), suitable instances are removed from O and the new cluster is created. We assume the availability of a supervisor that is able to label new faulty clusters, e.g., by providing the type of encountered fault. This allows us for creating online the fault dictionary. On the contrary, when the hypothesis H_0 is not rejected, Algorithm 2 returns an empty set (Line 32).

It is worth noting that the Mahalanobis distance cannot be considered to measure parameter vector proximities in O, since the distribution of elements in the outlier set is unknown (i.e., we cannot assume that $\hat{\theta}$s $\in O$ are Gaussian distributed as they are not). To address this issue, we defined the spatial–temporal norm on $\hat{\theta}_h, \hat{\theta}_j \in O$, inspired by the metric suggested in [42]

$$||\hat{\theta}_h - \hat{\theta}_j||_\lambda^2 = \lambda \frac{||\hat{\theta}_h - \hat{\theta}_j||^2}{2p} + (1-\lambda)\frac{|h-j|}{i}$$

where $||\cdot||$ is the Euclidean norm, i is the last batch of data considered, and $\lambda \in [0, 1]$ is a penalty factor balancing the spatial locality and the temporal one. A normalization procedure is required so that both the spatial and temporal components of the norm are constrained to the [0, 1] interval. The FDS algorithm adopts the online normalization procedure described in [43].

To select parameter vectors for the new clusters, we adopted the mountain method [44]–[46], which identifies the density center for the $\hat{\theta}$s $\in O$ (Lines 8–12). Finally, this algorithm estimates the density as

$$\Omega_{\text{RMM}}(c_j, \hat{\theta}_h; r) = \exp\left(-\frac{||\hat{\theta}_h - c_j||_\lambda^2}{2r^2}\right)$$

where $c_j \in \mathbb{R}^p$ is a center and r is an influence radius parameters. The algorithm iteratively approximates

$$c^* = \max_c \sum_{\hat{\theta}_h \in O} \Omega_{\text{RMM}}(c, \hat{\theta}_h, r).$$

The potential function Ω_{RMM} is robust to outliers (see [46] for a formal proof) and, since it decreases slowly when $||\hat{\theta}_h - c_j||_\lambda < r$ and fast if $||\hat{\theta}_h - c_j||_\lambda > r$, it defines a neighborhood around each class center c_j. For the purpose of the cluster creation, a center will be initialized for each of the parameter vectors $\hat{\theta}_h$s $\in O$. As described in [44], η_i of Algorithm 2 represents both a tolerance threshold for the convergence of the iterative procedure to identify the cluster center and the maximum error of the optimization procedure. As one might imagine that the method is rather sensitive to r, which highly influences the clustering results. Here, we suggested three different heuristics to identify a suitable value for the radius r:

1) power estimate using correlation [46];
2) median distance criterion [45];
3) maximum edge length of minimum spanning tree under the normal distribution hypothesis [47].

At the end of the mountain method, each parameter vector is associated with a set O_s (Lines 14 and 15) and $\tilde{O}$, the set characterized by the largest cardinality, is selected as a new candidate cluster.

To identify the cluster shape of $\tilde{O}$ (we do not have *a priori* information about the covariance matrix of the novel cluster), a minimum covariance determinant search method [48] is executed (Lines 16–29), i.e., a subset of elements $\bar{O} \subseteq \tilde{O}$ is selected such that the determinant of the parameter covariance is minimal. This method can be applied when the number of samples in $\tilde{O} \geq p$. When this condition is satisfied (Line 16), a new cluster is created: the mean and the covariance of the parameter vectors in $\bar{O}$ are computed, $n_{\Phi_{\phi+1}} = |\bar{O}|$, $t_{\Phi_{\phi+1}} = \max_{\hat{\theta}_h \in \bar{O}} h$, and the algorithm returns $\bar{O}$ (Line 27).

Algorithm 2 Fault Cluster Creation

1 Given an outlier set O
2 Set $\alpha_c \in (0, 1)$, η_i;
3 Compute D^p according to 15 ;
4 **if** $D^p > K_{\alpha_c}$ **then**
5 Set $c_h = \hat{\theta}_h$, $\forall \hat{\theta}_h \in O$ and $err \geq \eta_i$;
6 Compute r;
7 **while** $err \geq \eta_i$ **do**
8 **for** j *s.t.,* $\hat{\theta}_h \in O$ **do**
9 $\hat{c}_j \leftarrow c_j$;
10 $c_j \leftarrow \dfrac{\sum_{\hat{\theta}_h \in O} \Omega_{\text{RMM}}(c_j, \hat{\theta}_h; r)\hat{\theta}_h}{\sum_{\hat{\theta}_h \in O} \Omega_{\text{RMM}}(c_j, \hat{\theta}_h; r)}$;
11 **end**
12 $err = \max_k ||\hat{c}_j - c_j||_\lambda$;
13 **end**
14 Associate all centers c_j, c_h s.t. $||c_j - c_h||_\lambda \leq 2\eta_i$ to a set, creating the sets $O_1, \ldots, O_S$;
15 Let $\tilde{O} = \arg\max_{s \in \{1,\ldots,S\}} |O_s|$, i.e., the set with the largest cardinality ;
16 **if** $|\tilde{O}| \geq p$ **then**
17 Choose randomly $h = \frac{|\tilde{O}|+p+1}{2}$ elements in $\tilde{O}$ to define $\bar{O}$;
18 Set $S^* = \sum_{\hat{\theta}_k \in \bar{O}} \frac{(\hat{\theta}_k - c^*)(\hat{\theta}_k - c^*)^T}{h-1}$;
19 **while** $\bar{O} \neq \bar{O}'$ **do**
20 $\bar{O}' \leftarrow \bar{O}$;
21 **for** $\hat{\theta}_h \in \bar{O}$ **do**
22 $d(\hat{\theta}_k) = (\hat{\theta}_k - c^*)(S^*)^{-1}(\hat{\theta}_k - c^*)^T$;
23 **end**
24 $\bar{O} \leftarrow \arg\min_{O' \subseteq \tilde{O}, |O'|=h} \sum_{\hat{\theta}_k \in O'} d(\hat{\theta}_k)$;
25 $S^* \leftarrow \sum_{\hat{\theta}_k \in \bar{O}} \frac{(\hat{\theta}_k - c^*)(\hat{\theta}_k - c^*)^T}{h-1}$;
26 **end**
27 Return $\bar{O}$;
28 **else**
29 Return $\emptyset$;
30 **end**
31 **else**
32 Return $\emptyset$;
33 **end**

Otherwise, when $\tilde{O} < p$, the algorithm returns the empty set $\emptyset$ (Line 29).

Note that the algorithm requires at least $n_\Upsilon = p + 1$ parameter vectors to create a cluster. More parameter vectors would allow a better characterization of the cluster itself since the variance of the estimation of the mean and the covariance matrix scales asymptotically as $1/n_\Upsilon$. Moreover, as time passes, more and more parameter vectors are inserted into the outlier set. To reduce as much as possible the creation of false classes, we should consider an oblivion coefficient on the parameter vectors in the outlier set or mechanisms to discard the oldest ones (e.g., by setting a maximum value on the cardinality of the outlier set and keeping the new ones). The algorithm can be easily modified to take into account this case.

V. Experimental Result

The aim of this section is to evaluate the effectiveness of the proposed cognitive FDS. As we have observed, each state of the process (either nominal or faulty) is a cluster of parameter vectors: creation of the right number of clusters refers to the ability of the method to correctly identify the number of states the process explores. Likewise, an accurate aggregation of parameter vectors coming from the same state refers to the ability of correctly characterizing the operational state. As described in Section I, and to the best of our knowledge, no cognitive FDSs able to characterize the fault dictionary during the operational life are available in the literature. As a consequence, to compare the performance of the FDS, we consider algorithms designed to group unlabeled data, a task commonly addressed by clustering methods. We consider both offline clustering algorithms, such as the DBScan (DBS) [49], the affinity propagation (AP) [50], and the ECM [24]. DBS and AP process the whole data set and do not require *a priori* information about the number of clusters to be created, hence representing a relevant reference for the proposed FDS. On the contrary, ECM manages clusters with evolving strategies; the drawback here is that it requires parameter D_{thr}, which is strictly related to the number of clusters the algorithm will create during the operational life (such information is obviously unknown in real applications).

To evaluate the performance of the suggested method, we consider the following figures of merit:

1) n_c: the number of created clusters. It represents the number of states detected by the algorithm. When n_c equalizes the correct number of states, the algorithm operates well;
2) r: the percentage of experiments where the algorithm creates the correct number of clusters. Large values of r suggest that the fault diagnosis method is able to correctly characterize the number of process states;
3) a: the accuracy in associating a parameter vector to the correct cluster. It represents the ability to correctly identify the state in which the process is operating;
4) p_o: the percentage of outliers, i.e., the percentage of parameter vectors, which cannot be associated to any state. Large values of p_o imply that the algorithm is not able to associate parameter vectors to any cluster.

It is worth mentioning that the FDS requires an initial training phase. The FDS is trained on the training set and tested on a separate test set, while DBS, AP, and ECM are applied to the whole training + test set (but their performance are evaluated only on the test set). Since ECM and AP do not generate outliers, p_o is not provided for them.

We considered two different hierarchies of model family $\mathcal{M}(\theta)$:

1) the autoregressive with exogenous input ARX(na, nb) linear model family, where na and nb are the auto-regressive and exogenous orders, respectively. Here, the

$p = \mathrm{na} + \mathrm{nb}$ dimensional parameter vector $\theta \in \mathbb{R}^p$ is

$$\theta = (\theta_1, \ldots, \theta_{\mathrm{na}}\ \theta_{\mathrm{na}+1}, \ldots, \theta_{\mathrm{na}+\mathrm{nb}})$$

2) the reservoir network (RN) [51] model defined as

$$\begin{aligned} x(t) &= g\left(Wx(t-1) + W_{in}u(t)\right) \\ \hat{y}(t) &= \theta x(t) \end{aligned}$$

where $\hat{y}(t) \in \mathbb{R}$ is the prediction value at time $t \in \mathbb{N}$, $u(t) \in \mathbb{R}^m$ is the input observation vector at time t, $x(t) \in \mathbb{R}^p$ is the internal state of the network at time t, $W \in \mathbb{R}^{p\times p}$ is the internal weight matrix, and $W_{in} \in \mathbb{R}^{p\times m}$ is an input weight matrix, both randomly chosen. $g : \mathbb{R}^p \to \mathbb{R}^p$ is an activation function (e.g., $g_i(\cdot) = \tanh(\cdot), i \in \{1, \ldots, p\}$) and $\theta \in \mathbb{R}^p$ is an output weight vector to be learned (model parameter vector).

We considered ARX and RN model families since they satisfy the hypotheses required by the theoretical framework described in Section II. The structural risk is the squared error; the Bayesian information criterion [52] was considered to identify model orders. In the following, batches of $N = 400$ not overlapping data are considered to estimate the parameters of the approximating models. The proposed FDS has been developed in MATLAB and can be freely downloaded from [53] and [54].

The performance of the proposed FDS system has been compared with those of DBS, AP, and ECM methods applied to three different applications: a synthetic one, a simulation of the Barcelona water distribution network (BWDN) and a real-world application related to rock collapse forecasting. On the aforementioned applications, faults are of abrupt type as requested by the proposed FDS. Three applications are detailed in the sequel.

A. General Remarks on the FDS Method

Key parameters describing the FDS algorithm are given in Table I. In particular few parameters are described as follows:

1) the spatial confidence α_s has been set to 0.03 (3). This parameter controls the rate of structural outliers generated by the FDS. Large values of α_s would create more compact clusters and be sensitive to new states, at the expenses of a larger outlier set. On the contrary, small values of α_s would reduce the number of outliers at the expenses of a reduced sensitivity in identifying new states;
2) the temporal threshold η_t has been set to one, meaning that cluster statistics in (8) are updated when two consecutive parameter vectors are inserted in the same cluster. Larger values of η_t update the cluster statistics with less restrictive conditions. $\eta_t = 1$ represents a conservative choice for this parameter;
3) the merging confidence α_m has been set to 0.05. It represents the confidence of the hypothesis test designed to assess whether two clusters need to be merged or not;
4) the cluster creation confidence α_c has been set to 0.1. It represents the confidence of the KS hypothesis test, meant to assess if a new cluster must be created by looking at the distribution of the parameter vectors in the outlier set.

TABLE I

PARAMETERS OF THE PROPOSED FDS

Spatial confidence	$\alpha_s = 0.03$
Temporal threshold	$\eta_t = 1$
Merging confidence	$\alpha_m = 0.05$
KS-test confidence	$\alpha_c = 0.1$
Spatial-temporal penalization	$\lambda = 0.5$
Mountain method threshold	$\eta_i = 10^{-6}$

Since the FDS creates clusters with as low as $p+1$ parameter vectors (required by the minimum covariant determinant procedure, see Section IV for details), we set the DBS parameter minPts to $p + 1$ to have a fair comparison. Parameter ε of DBS has been set using the heuristics described in [49]. The ECM parameter D_{thr} was set to 0.1, as suggested in [24].

B. APP D1: Synthetic Application

Synthetic data are generated according to model

$$y(t) = \sin\left(a_1 y(t-1) + a_2 y(t-2) + b_1 u(t-1)\right) + d(t) \tag{16}$$

where $a_1 = 0.1$, $a_2 = 0.2$, $b_1 = -0.1$, and $d(t) \sim \mathcal{N}(0, 10^{-4})$. The exogenous input follows the model

$$u(t) = 0.4u(t-1) + \epsilon(t)$$

with $\epsilon(t) \sim \mathcal{N}(0, 1)$.

The length of each experiment is 60 300 samples with the first 24 120 ones used to train the FDS. Faults affecting the system have been modeled as abrupt changes in the parameters of (16). This models the situation where a fault affecting the system induces a change in the dynamics of the relationship between input and output. The first fault affects the system in sample interval [24 120, 36 180], inducing an abrupt change, which shifts the parameters from $\theta = (a_1\ a_2\ b_1)$ to $\theta_\delta = (1 + \delta)\theta$, δ being a positive scalar controlling the intensity of the perturbation. Afterward, the data-generating process returns to the nominal state. Then, another fault affects the system in sample interval [48 240, 60 300], inducing a change in the parameters from θ to $\theta_\delta = (1-\delta)\theta$. As a consequence, the total number of states for this application is three (i.e., the nominal state and the two faulty ones). We considered different scenarios for this application by taking into account abrupt changes in the parameters with magnitude δ ranging from 0.01 to 0.3. For each scenario, we generated 200 experiments; averaged results are presented in Tables II and III.

In particular, Table II shows the number of created clusters n_c for the considered algorithms, model hierarchies, and fault magnitudes. As expected, the ability to create the correct number of clusters increases with the magnitude of δ (a strong fault is easy to be identified). Interestingly, the FDS with ARX is able to correctly create three clusters even with very low fault magnitudes (e.g., $\delta = 0.015$). ECM creates an excessive number of clusters making this algorithm not useful in this application. The reason of this behavior resides in the incorrect setting of D_{thr} [49]. Unfortunately, as explained above, it is hard to set this parameter for fault diagnosis purpose, since

TABLE II

NUMBER OF CLUSTERS CREATED FOR THE CONSIDERED APPLICATIONS. AVERAGE VALUES IS GIVEN AND STANDARD DEVIATION IN BRACKETS

		Fault	n_c			
			FDS	ECM	DBS	AP
APP D1 (SYN)	ARX	$\delta = 0.010$	1.8(0.8)	120.1(3.6)	1.0(0.1)	12.7(1.1)
		$\delta = 0.015$	3.3(0.5)	118.3(3.7)	1.0(0.2)	12.7(1.1)
		$\delta = 0.020$	3.2(0.4)	113.8(3.7)	1.1(0.4)	12.9(1.1)
		$\delta = 0.025$	3.2(0.5)	108.8(3.7)	1.8(0.7)	12.9(1.1)
		$\delta = 0.050$	3.2(0.4)	88.5(3.7)	3.0(0.2)	11.6(1.1)
		$\delta = 0.100$	3.2(0.5)	60.7(3.3)	3.0(0.0)	7.1(0.8)
		$\delta = 0.200$	3.2(0.4)	33.8(2.8)	3.0(0.0)	3.8(0.4)
		$\delta = 0.300$	3.1(0.3)	21.5(2.2)	3.0(0.0)	3.0(0.0)
	RN	$\delta = 0.010$	1.0(0.1)	89.4(20.6)	1.0(0.0)	11.2(2.0)
		$\delta = 0.015$	1.0(0.2)	90.2(21.2)	1.0(0.1)	11.0(2.0)
		$\delta = 0.020$	1.0(0.2)	88.0(22.5)	1.0(0.1)	11.2(2.1)
		$\delta = 0.025$	1.1(0.4)	90.6(22.0)	1.0(0.0)	11.1(1.9)
		$\delta = 0.050$	1.5(0.8)	88.8(22.1)	1.0(0.2)	10.9(2.0)
		$\delta = 0.100$	2.4(1.0)	84.9(18.9)	1.2(0.5)	10.1(2.2)
		$\delta = 0.200$	2.7(0.9)	68.7(22.0)	1.9(1.0)	8.1(2.9)
		$\delta = 0.300$	2.6(0.9)	52.1(23.3)	2.3(0.9)	6.6(3.1)
APP D2 (BWDN)	ARX	$BW1$	2	38	1	4
		$BW2$	3	57	1	6
		$BW3$	4	47	2	4
		$BW4$	5	59	2	6
APP D3 (RIALBA)	ARX	$R1$	2	48	1	10
		$R2$	3	39	1	8

it is related to the number of clusters to be created, which is obviously unknown *a priori*. Interestingly, both DBS and AP with ARX are able to create the correct number of clusters, for large δ magnitudes, i.e., $\delta \geq 0.05$ and $\delta \geq 0.3$, respectively. Despite the evolving approach, the proposed FDS with ARX is more effective in creating the correct number of clusters once compared with nonevolving algorithms, such as the DBS and the AP even for small δs. The rationale behind this refers to the fact that the FDS is able to simultaneously consider both temporal and spatial dependencies among parameter vectors.

RNs provide lower performance than ARX. The reason of this behavior can be associated to the fact that the performance of RNs is highly influenced by the choice of the random network topology. In fact, training the network topology is entirely based on nominal state samples. This leads to an RN modeling the nominal state, but does not necessarily guarantee the ability to identify new states during the operational life. However, the ability to create the correct number of clusters increases with δ and the FDS with RN is able to identify the correct number of faults with magnitude $\delta \geq 0.2$.

Then, to evaluate the ability to correctly identify the states where the process operates over time, we focus only on those experiments for which the number of created clusters is correct. Table III shows r, a, and p_0 for ARX, RNs, and fault magnitudes, when the number of clusters created by the algorithm is correct (i.e., $n_c = 3$ for APP D1).

As expected, the FDS improves its performance both in terms of percentage of experiments, which identified the correct number of clusters r, and in terms of the classification accuracy a as the magnitude of the fault increases. Interestingly, when $\delta < 0.015$, the FDS with ARX reduces its effectiveness in the clustering (i.e., $r = 12.0\%$ and $a = 51.7\%$) meaning that small fault magnitudes represent challenging situations for the proposed approach. In our opinion, this behavior is due to the fact that the neighborhood of probability $1-\alpha_s$ induced by the covariance matrix Σ_N includes also some faulty states when $\delta \leq 0.01$.

Furthermore, the analysis of p_0 allows us to evaluate the effect of the choice of the FDS parameters on performance. Specifically, as explained in the previous section, the parameter α_s controls the percentage of structural outliers of the FDS and this is particularly evident by the values of p_o in Table III, which are in line with what expected from the theory. On the contrary, the percentage of outliers of DBS decreases, when the fault magnitude increases. This is reasonable since the method does not contemplate a fixed percentage of structural outliers.

By inspecting accuracy a, we observe that the FDS with ARX provides higher performance than the one with RN in the small perturbation case ($\delta \leq 0.025$). As the magnitude δ increases, there is no strong evidence for selecting a specific model family. Nevertheless, the standard deviation of the accuracy of ARX model is lower than the RN model one. This behavior is in line with the difficulties in selecting the RN topology following the discussions given for Table II.

As expected, non evolving clustering methods, such as DBS or AP, provide higher performance than FDS when $\delta = 0.3$. This is reasonable since these algorithms work in an offline way, by analyzing the whole data set at once. On the contrary, the proposed FDS provides better performance than DBS and AP with small values of δ, making it suitable to manage subtle and not evident faults. Even in this case, the reason of this behavior resides in the ability of the method to exploit temporal dependencies among parameter vectors during the

TABLE III

EXPERIMENTAL RESULTS FOR THE CONSIDERED APPLICATIONS. AVERAGE VALUE IS GIVEN AND STANDARD DEVIATION IN BRACKETS

		Fault	FDS			ECM		DBS			AP	
			r	a	p_o	r	a	r	a	p_o	r	a
APP D1 (SYN)	ARX	$\delta = 0.010$	12.0	51.7(9.3)	3.4(3.8)	0.0	N.a.	0.0	N.a.	N.a.	0.0	N.a.
		$\delta = 0.015$	72.5	84.5(9.6)	2.7(2.8)	0.0	N.a.	0.0	N.a.	N.a.	0.0	N.a.
		$\delta = 0.020$	82.0	95.4(3.5)	3.1(3.3)	0.0	N.a.	1.5	55.9(12.0)	6.7(2.9)	0.0	N.a.
		$\delta = 0.025$	83.5	96.5(2.8)	3.0(2.8)	0.0	N.a.	13.0	92.1(7.3)	5.6(2.4)	0.0	N.a.
		$\delta = 0.050$	82.0	96.2(3.4)	3.5(3.4)	0.0	N.a.	97.5	97.6(1.8)	2.4(1.8)	0.0	N.a.
		$\delta = 0.100$	81.5	96.7(3.1)	2.6(3.1)	0.0	N.a.	100.0	99.4(0.8)	0.6(0.8)	0.0	N.a.
		$\delta = 0.200$	86.5	96.5(2.9)	2.6(2.8)	0.0	N.a.	100.0	100.0(0.0)	0.0(0.2)	17.5	100.0(0.0)
		$\delta = 0.300$	88.0	96.8(2.8)	2.4(2.8)	0.0	N.a.	100.0	100.0(0.0)	0.0(0.0)	100.0	100.0(0.0)
	RN	$\delta = 0.010$	0.0	N.a.	N.a.	0.0	N.a.	0.0	N.a.	N.a.	0.0	N.a.
		$\delta = 0.015$	0.0	N.a.	N.a.	0.0	N.a.	0.0	N.a.	N.a.	0.0	N.a.
		$\delta = 0.020$	0.5	66.7(0.0)	1.1(0.0)	0.0	N.a.	0.0	N.a.	N.a.	0.0	N.a.
		$\delta = 0.025$	3.5	63.0(23.0)	3.0(3.0)	0.0	N.a.	0.0	N.a.	N.a.	0.0	N.a.
		$\delta = 0.050$	16.5	80.9(16.8)	3.7(3.4)	0.0	N.a.	1.5	97.8(1.1)	2.2(1.1)	0.0	N.a.
		$\delta = 0.100$	45.0	90.9(10.5)	3.9(4.4)	0.0	N.a.	6.5	97.9(2.6)	2.0(2.7)	0.0	N.a.
		$\delta = 0.200$	60.5	94.3(7.0)	3.4(4.6)	0.0	N.a.	38.5	98.5(3.6)	1.1(1.7)	4.0	100.0(0.0)
		$\delta = 0.300$	58.5	95.3(6.8)	3.0(3.5)	0.0	N.a.	63.5	99.3(1.5)	0.7(1.5)	25.5	100.0(0.0)
APP D2 (BWDN)	ARX	$BW1$	100	95.5	0.0	0	N.a.	0	N.a.	N.a.	0	N.a.
		$BW2$	100	81.8	0.0	0	N.a.	0	N.a.	N.a.	0	N.a.
		$BW3$	100	81.5	0.0	0	N.a.	100	56.9	4.0	0	N.a.
		$BW4$	100	80.5	3.4	0	N.a.	0	N.a.	N.a.	0	N.a.
APP D3 (RIALBA)	ARX	$R1$	100	90.6	3.8	0	N.a.	0	N.a.	N.a.	0	N.a.
		$R2$	100	92.5	0.0	0	N.a.	0	N.a.	N.a.	0	N.a.

operational life (while not evolving algorithms do not exploit time dependencies in the clustering phase). ECM was never able to correctly identify the number of clusters, in line with comments following Table II.

We also performed a robustness analysis to evaluate the effects of variations of the main parameters of the FDS, i.e., α_s, α_m, η_t, and λ, on the considered figures of merit. In the considered scenario APP D1, which is characterized by a stationary process affected by abrupt changes, parameter α_s revealed to be the most sensitive one and its behavior is deeply investigated in the sequel. Fig. 2(a) and (b) shows how the figures of merit a, p_0, r, and n_c range with α_s ranging in the interval $[2.5E{-}3; 2.5E{-}1]$. As expected, p_0 increases with α_s and this is quite obvious since we are creating clusters that are more and more compact. For the considered scenario, $\alpha_s = 0.025$ guarantees the highest value of r. Interestingly, lower values of α_s create a reduced number of clusters, while larger ones create an excessive number of clusters. This behavior is evident by looking at the values of n_c in Fig. 2(b). The behavior of the classification accuracy a is particularly interesting: small values of α_s create very large clusters, hence possibly misclassifying estimated parameters that belong to a different state (e.g., a faulty one); on the contrary, large values of α_s create very small clusters, hence generating many outliers (and this is evident by looking at the behavior of p_0 when α_s increases).

C. APP D2: BWDN

The second testbed refers to data generated from the BWDN simulator [55]. By relying on a network of 17 tanks, 26 pumps, 35 valves, and nine external sources of the BWDN, this simulator allows to artificially inject faults in a specific flow sensor of the network (i.e., the `iOrioles` pump), by specifying the fault signature, the fault magnitude, and the fault time horizon. Four different scenarios have been considered:

- BW1 An abrupt additive fault affecting the measurements of the `iOrioles` pump is injected in sample interval [9546, 17 472]. The magnitude of the additive fault is −20% of the signal dynamic (i.e., the range between the maximum and minimum value of the signal). The length of the data set is 17 472 samples;
- BW2 A sensor degradation fault is injected in sample interval [18 282, 26 208]. This fault consists in an additive Gaussian noise with zero mean and standard deviation equal to 30% of the signal one. The length of the data set is 26 208 samples. The first 17 472 samples are equal to the BW1 case;
- BW3 A stuck-at fault is injected in sample interval [27 018, 34 944]. The length of the data set is 34944 samples. The first 26 208 samples are equal to the BW2 case;
- BW4 An abrupt additive fault affecting the measurements of the `iOrioles` pump is injected in sample interval [35 754, 43 680]. The magnitude of the additive fault is 20% of the range of the signal. The length of the data set is 43 680 samples. The first 34 944 samples are equal to the BW3 case.

The FDS has been trained on the first 8736 samples (representing one year of observations in the BWDN simulator) in all the four considered scenarios; as a reference model we consider the ARX.

Results given in Table II are particularly interesting and show how the proposed FDS is able to correctly identify the

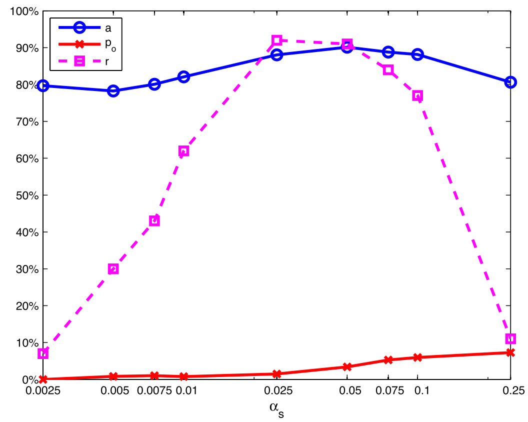

(a)

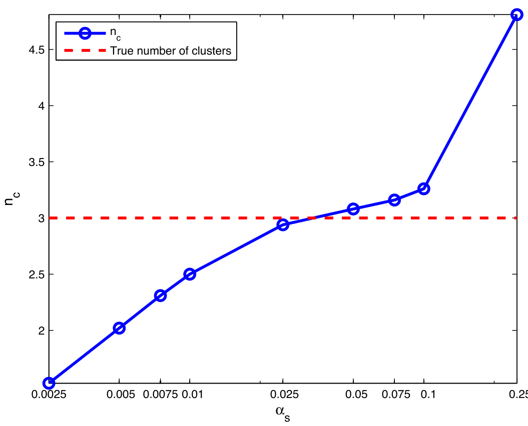

(b)

Fig. 2. Robustness analysis result for α_s. (a) Average accuracy a, outlier percentage p_o, and percentage of experiments where the algorithm creates the correct number of clusters r are reported for the experiments where $n_c = 3$. (b) Average number of cluster n_c created with different values of α_s.

number of clusters in all the four considered scenarios. All other considered methods do not identify the correct number of clusters (with the exception of AP in the BW3 scenario). In line with the synthetic application experiments, AP and DBS usually detect a smaller (1–2) and larger (4–6) number of clusters than necessary, respectively, while ECM creates an excessive number of clusters, i.e., from 38 to 59. These results corroborate the ability of the proposed FDS method to correctly characterize the states explored by the process over time.

In Table III, the value of r is either zero or 100, since here we are considering a single experiment. FDS accuracy decreases from 95.5% in BW1 to 81.8% in BW2, while there is no further significant reduction in accuracy in the other scenarios. In our opinion in scenario BW2, the injected degradation fault is particularly hard to be detected, since its effect on the estimated parameter vectors is not as evident as those induced by the other considered faults.

D. APP D3: A Monitoring System for Landslide Forecasting

In this application, data are gathered from a monitoring system for landslide forecasting, [56] deployed at the Towers of Rialba site in Northern Italy. The data set, available at [53], consisting in 35 652 samples, has been acquired in 2011, with

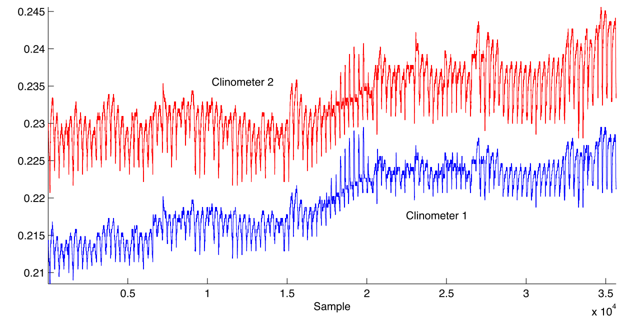

Fig. 3. APP D3: the measurements acquired from two clinometers of the monitoring system deployed at the Towers of Rialba.

a sampling period of 5 min. This data set, which is shown in Fig. 3, collects measurements coming from two clinometers.

Two different scenarios have been considered:

- R1 An abrupt additive fault affecting the measurements of the clinometer, regarded as output, is injected in sample interval [17 468, 24 956]. The magnitude of the additive fault is −20% of the signal dynamics;
- R2 The first 24956 samples are equal to the R1 case. Then, a degradation fault is injected in the same clinometer in sample interval [28164, 35652]. The degradation fault consists in an additive Gaussian noise with zero mean and standard deviation equal to 30% of the signal one.

We emphasize that, to ease the comparison, R1 and R2 in APP D3 correspond to BW1 and BW2 in APP D2, respectively. In this application, the first 14260 samples have been used to train the FDS. The chosen model hierarchy was ARX.

Experimental results on this application are particularly interesting since data are coming from a real monitoring system.

By looking at Table II, we observe that the number of states of the process is correctly recognized by the FDS in both scenarios whereas other methods are never able to create the correct number of clusters. These results are in line with APP D1-D2: AP and ECM are creating more clusters than necessary and DBS is creating a single cluster.

The FDS accuracy in R1 and R2, presented in Table III, are similar (i.e., 90.6% in R1 and 92.5% in R2), showing that we are able to deal effectively with multiple faults. With respect to the BWND application, here we do not have a decrease in performance as the degradation fault appears, suggesting that, in this application, the effect of the degradation fault is more easy to be perceived by the FDS.

VI. Conclusion

This paper presents an evolving mechanism for cognitive fault diagnosis able to detect and cluster faults by characterizing the nominal state and the fault dictionary (initially empty) during the operational phase. The novelty of the proposed approach resides in the evolving mechanisms and the theoretically grounded framework that allows to work in the space of linear approximating models, even if the system under investigation is nonlinear. The cognitive approach allows us to characterize the faults during the operational phase by introducing clusters in the parameter vector space and updating them in an evolving manner. The experimental section shows the effectiveness of the proposed solution once compared with the existing clustering algorithm applied to both synthetic and real data. Results show the better ability of the proposed method over the ones present in the literature to correctly identify the states the process encounters over time.

REFERENCES

[1] R. Isermann, *Fault-Diagnosis Systems: An Introduction from Fault Detection to Fault Tolerance*. New York, NY, USA: Springer-Verlag, 2006.

[2] J. Gertler, *Fault Detection and Diagnosis in Engineering Systems*. Boca Raton, FL, USA: CRC Press, 1998.

[3] J. B. Comly, P. P. Bonissone, and M. E. Dausch, *Fuzzy Logic for Fault Diagnosis*. Schenectady, NY, USA: GE Research & Development Center, 1990.

[4] V. Venkatasubramanian, R. Rengaswamy, S. N. Kavuri, and K. Yin, "A review of process fault detection and diagnosis: Part III: Process history based methods," *Comput. Chem. Eng.*, vol. 27, no. 3, pp. 327–346, Mar. 2003.

[5] R. Isermann and P. Ballé, "Trends in the application of model-based fault detection and diagnosis of technical processes," *Control Eng. Pract.*, vol. 5, no. 5, pp. 709–719, May 1997.

[6] M. A. Demetriou and M. M. Polycarpou, "Incipient fault diagnosis of dynamical systems using online approximators," *IEEE Trans. Autom. Control*, vol. 43, no. 11, pp. 1612–1617, Nov. 1998.

[7] J. Farrell, T. Berger, and B. D. Appleby, "Using learning techniques to accommodate unanticipated faults," *IEEE Control Syst.*, vol. 13, no. 3, pp. 40–49, Jun. 1993.

[8] M. Fochem, P. Wischnewski, and R. Hofmeier, "Quality control systems on the production line of tape deck chassis using self organizing feature maps," in *Proc. Eur. Symp. Appl. Intell. Technol.*, 1997, pp. 9–13.

[9] D. L. Yu, J. B. Gomm, and D. Williams, "Sensor fault diagnosis in a chemical process via RBF neural networks," *Control Eng. Pract.*, vol. 7, no. 1, pp. 49–55, Jan. 1999.

[10] A. B. Trunov and M. M. Polycarpou, "Automated fault diagnosis in nonlinear multivariable systems using a learning methodology," *IEEE Trans. Neural Netw.*, vol. 11, no. 1, pp. 91–101, Jan. 2000.

[11] Y.-C. Huang, "Evolving neural nets for fault diagnosis of power transformers," *IEEE Trans. Power Del.*, vol. 18, no. 3, pp. 843–848, Jul. 2003.

[12] B. S. Yang, T. Han, and Y. S. Kim, "Integration of ART-Kohonen neural network and case-based reasoning for intelligent fault diagnosis," *Expert Syst. Appl.*, vol. 26, no. 3, pp. 387–395, Apr. 2004.

[13] J. Zhang and A. J. Morris, "On-line process fault diagnosis using fuzzy neural networks," *Intell. Syst. Eng.*, vol. 3, no. 1, pp. 37–47, 1994.

[14] X. Lou and K. A. Loparo, "Bearing fault diagnosis based on wavelet transform and fuzzy inference," *Mech. Syst. Signal Process.*, vol. 18, no. 5, pp. 1077–1095, Sep. 2004.

[15] M. Seera, C. P. Lim, D. Ishak, and H. Singh, "Fault detection and diagnosis of induction motors using motor current signature analysis and a hybrid FMM–CART model," *IEEE Trans. Neural Netw. Learn. Syst.*, vol. 23, no. 1, pp. 97–108, Jan. 2012.

[16] Y.-C. Huang, H.-T. Yang, and C.-L. Huang, "Developing a new transformer fault diagnosis system through evolutionary fuzzy logic," *IEEE Trans. Power Del.*, vol. 12, no. 2, pp. 761–767, Apr. 1997.

[17] R. Naresh, V. Sharma, and M. Vashisth, "An integrated neural fuzzy approach for fault diagnosis of transformers," *IEEE Trans. Power Del.*, vol. 23, no. 4, pp. 2017–2024, Oct. 2008.

[18] H. C. Kuo and H. K. Chang, "A new symbiotic evolution-based fuzzy-neural approach to fault diagnosis of marine propulsion systems," *Eng. Appl. Artif. Intell.*, vol. 17, no. 8, pp. 919–930, Dec. 2004.

[19] A. Joentgen, L. Mikenina, R. Weber, A. Zeugner, and H. J. Zimmermann, "Automatic fault detection in gearboxes by dynamic fuzzy data analysis," *Fuzzy Sets Syst.*, vol. 105, no. 1, pp. 123–132, Jul. 1999.

[20] R. K. Aggarwal, Q. Y. Xuan, A. T. Johns, F. Li, and A. Bennett, "A novel approach to fault diagnosis in multicircuit transmission lines using fuzzy ARTmap neural networks," *IEEE Trans. Neural Netw.*, vol. 10, no. 5, pp. 1214–1221, Sep. 1999.

[21] C. Alippi, M. Roveri, and F. Trovò, "A 'learning from models' cognitive fault diagnosis system," in *Artificial Neural Networks and Machine Learning–ICANN* (Lecture Notes in Computer Science). New York, NY, USA: Springer-Verlag, 2012, pp. 305–313.

[22] R. Xu and D. Wunsch, *Clustering*, vol. 10. New York, NY, USA: Wiley, 2008.

[23] O. Nasraoui and C. Rojas, "Robust clustering for tracking noisy evolving data streams," in *Proc. SIAM Int. Conf. Data Mining*, 2006, pp. 80–99.

[24] Q. Song and N. Kasabov, "ECM—A novel on-line, evolving clustering method and its applications," in *Proc. Conf. ANNES*, 2001, pp. 87–92.

[25] P. P. Angelov, P. Angelov, D. P. Filev, and N. Kasabov, *Evolving Intelligent Systems: Methodology and Applications*, vol. 12. New York, NY, USA: Wiley, 2010.

[26] A. Rosich, R. Sarrate, V. Puig, and T. Escobet, "Efficient optimal sensor placement for model-based FDI using an incremental algorithm," in *Proc. 46th IEEE Conf. Decision Control*, Dec. 2007, pp. 2590–2595.

[27] M. Krysander and E. Frisk, "Sensor placement for fault diagnosis," *IEEE Trans. Syst., Man Cybern., A, Syst. Humans*, vol. 38, no. 6, pp. 1398–1410, Nov. 2008.

[28] Y. Ding, P. Kim, D. Ceglarek, and J. Jin, "Optimal sensor distribution for variation diagnosis in multistation assembly processes," *IEEE Trans. Robot. Autom.*, vol. 19, no. 4, pp. 543–556, Aug. 2003.

[29] A. Khan and D. Ceglarek, "Sensor optimization for fault diagnosis in multi-fixture assembly systems with distributed sensing," *J. Manuf. Sci. Eng.*, vol. 122, no. 1, pp. 215–226, 2000.

[30] C. Alippi, S. Ntalampiras, and M. Roveri, "A cognitive fault diagnosis system for distributed sensor networks," *IEEE Trans. Neural Netw. Learn. Syst.*, vol. 24, no. 8, pp. 1213–1226, Aug. 2013.

[31] L. Ljung, *System Identification*. New York, NY, USA: Wiley, 1999.

[32] G. B. Huang, Q. Y. Zhu, and C. K. Siew, "Extreme learning machine: Theory and applications," *Neurocomputing*, vol. 70, nos. 1–3, pp. 489–501, Dec. 2006.

[33] B. Schrauwen, D. Verstraeten, and J. Van Campenhout, "An overview of reservoir computing: Theory, applications and implementations," in *Proc. Eur. Symp. Artif. Neural Netw.*, 2007, pp. 471–482.

[34] L. Ljung and P. E. Caines, "Asymptotic normality of prediction error estimators for approximate system models," in *Proc. IEEE Conf. Decision Control Including 17th Symp. Adapt. Process.*, vol. 17. Jan. 1978, pp. 927–932.

[35] L. Ljung, "Convergence analysis of parametric identification methods," *IEEE Trans. Autom. Control*, vol. 23, no. 5, pp. 770–783, Oct. 1978.

[36] R. A. Johnson and D. W. Wichern, *Applied Multivariate Statistical Analysis*, vol. 4. Upper Saddle River, NJ, USA: Prentice-Hall, 2002.

[37] P. Pébay, "Formulas for robust, one-pass parallel computation of covariances and arbitrary-order statistical moments," Sandia Nat. Lab., Albuquerque, NM, USA, Sandia Rep. SAND2008-6212, 2008.

[38] R. Saunders and P. Laud, "The multidimensional Kolmogorov goodness-of-fit test," *Biometrika*, vol. 67, no. 1, p. 237, 1980.

[39] A. N. Kolmogorov, "Sulla determinazione empirica di una legge di distribuzione," *Giornale Inst. Italiano Attuari*, vol. 4, no. 1, pp. 83–91, 1933.

[40] N. Smirnov, "Table for estimating the goodness of fit of empirical distributions," *Ann. Math. Statist.*, vol. 19, no. 2, pp. 279–281, Jun. 1948.

[41] A. Blum, "Random projection, margins, kernels, and feature-selection," in *Subspace, Latent Structure and Feature Selection*. New York, NY, USA: Springer-Verlag, 2006, pp. 52–68.

[42] I. Žliobaitė, "Combining similarity in time and space for training set formation under concept drift," *Intell. Data Anal.*, vol. 15, no. 4, pp. 589–611, Jun. 2011.

[43] S. Jaiyen, C. Lursinsap, and S. Phimoltares, "A very fast neural learning for classification using only new incoming datum," *IEEE Trans. Neural Netw.*, vol. 21, no. 3, pp. 381–392, Mar. 2010.

[44] R. R. Yager and D. P. Filev, "Approximate clustering via the mountain method," *IEEE Trans. Syst., Man Cybern.*, vol. 24, no. 8, pp. 1279–1284, Aug. 1994.

[45] C. W. Wu, J. L. Chen, and J. H. Wang, "Self-organizing mountain method for clustering," in *Proc. IEEE Int. Conf. Syst., Man, Cybern.*, vol. 4. Oct. 2001, pp. 2434–2438.

[46] M. S. Yang and K. L. Wu, "A similarity-based robust clustering method," *IEEE Trans. Pattern Anal. Mach. Intell.*, vol. 26, no. 4, pp. 434–448, Apr. 2004.

[47] M. D. Penrose, "Extremes for the minimal spanning tree on normally distributed points," *Adv. Appl. Probab.*, vol. 30, no. 3, pp. 628–639, 1998.

[48] J. Hardin and D. M. Rocke, "Outlier detection in the multiple cluster setting using the minimum covariance determinant estimator," *Comput. Statist. Data Anal.*, vol. 44, no. 4, pp. 625–638, 2004.

[49] M. Ester, H.-P. Kriegel, J. Sander, and X. Xu, "A density-based algorithm for discovering clusters in large spatial databases with noise," in *Proc. 2nd Int. Conf. KDD*, 1996, pp. 1–6.

[50] B. J. Frey and D. Dueck, "Clustering by passing messages between data points," *Science*, vol. 315, no. 5814, pp. 972–976, 2007.

[51] H. Jaeger, "Tutorial on training recurrent neural networks, covering BPPT, RTRL, EKF and the echo state network approach," GMD-Forschungszentrum Informationstechnik, Postfach, Germany, GMD Rep. 159, 2002.

[52] G. Schwarz, "Estimating the dimension of a model," *Ann. Statist.*, vol. 6, no. 2, pp. 461–464, 1978.

[53] (2013, Jun.). *Matlab Fds Toolbox and Dataset* [Online]. Available: http://home.deib.polimi.it/roveri/software

[54] (2013, Jun.). *Isense Project Website* [Online]. Available: http://www.i-sense.org/

[55] E. Caini, V. P. Cayuela, and G. C. Gennari, "Development of a simulation environment for water drinking networks: Application to the validation of a centralized MPC controller for the barcelona case study," Univ. Politècnica de Catalunya, Barcelona, Spain, Tech. Rep. IRI-TR-09-03, 2009.

[56] C. Alippi, R. Camplani, C. Galperti, A. Marullo, and M. Roveri, "A high frequency sampling monitoring system for environmental and structural applications," *ACM Trans. Sensor Netw.*, vol. 9, no. 4, pp. 41–32, Jul. 2013.